

## Preliminary results on Saturn's inner plasmasphere as observed by Cassini: Comparison with Voyager

E. C. Sittler Jr.,<sup>1</sup> M. Thomsen,<sup>2</sup> D. Chornay,<sup>1</sup> M. D. Shappirio,<sup>1</sup> D. Simpson,<sup>1</sup> R. E. Johnson,<sup>3</sup> H. T. Smith,<sup>3</sup> A. J. Coates,<sup>4</sup> A. M. Rymer,<sup>4</sup> F. Crary,<sup>5</sup> D. J. McComas,<sup>5</sup> D. T. Young,<sup>5</sup> D. Reisenfeld,<sup>6</sup> M. Dougherty,<sup>7</sup> and N. Andre<sup>8</sup>

Received 7 February 2005; revised 16 March 2005; accepted 30 March 2005; published 15 June 2005.

[1] We present an analysis of Saturn's inner plasmasphere as observed by the Cassini Plasma Spectrometer (CAPS) experiment during Cassini's initial entry into Saturn's magnetosphere when the spacecraft was inserted into orbit around Saturn. The ion fluxes are divided into two sub-groups: protons and water group ions. We present the relative amounts of these two groups and the first estimates of their fluid parameters: ion density, flow velocity and temperature. We also compare this data with electron plasma measurements. Within the plasmasphere and inside of Enceladus' orbit, water group ions are about a factor of  $\sim 10$  greater than protons in number with number densities exceeding  $40 \text{ cm}^{-3}$ . Within this inner region the spacecraft acquires a negative potential so that the electron density is underestimated. The electron and proton temperatures, which could not be measured in this region by Voyager, are  $T \sim 2 \text{ eV}$  at  $L \sim 3$ . Also, within this inner region the protons, because of a negative spacecraft potential, appear to be super-corotating. By enforcing the condition that protons and water group ions are co-moving we may be able to acquire an independent estimate of the spacecraft potential relative to that estimated when comparing ion-electron measurements. Using our estimates of plasma properties, we estimate the importance of the rotating plasma on the stress balance equation for the inner magnetosphere and corresponding portion of the ring current. **Citation:** Sittler, E. C., Jr., et al. (2005), Preliminary results on Saturn's inner plasmasphere as observed by Cassini: Comparison with Voyager, *Geophys. Res. Lett.*, *32*, L14S07, doi:10.1029/2005GL022653.

### 1. Introduction

[2] The inner magnetosphere of Saturn was first probed by the Pioneer 11 spacecraft in 1979 with an equatorial trajectory along the noon meridian with closest approach inside of Mimas' orbit, near dipole  $L \sim 3$  [Wolfe *et al.*,

1980]. The ion measurement results reported by Frank *et al.* [1980], were interpreted to be dominated by  $\text{O}^{++}$ . Then the Voyager 1 and 2 spacecraft had close encounters with Saturn in 1980 and 1981, respectively. The Voyager 1 trajectory was confined outside  $L \sim 3.4$  with a ring plane crossing at Dione's L shell ( $L \sim 6.3$ ), while Voyager 2 approached at mid-latitudes with a ring plane crossing inside the G-ring ( $L \sim 2.7$ ). Initial plasma results were presented by Bridge *et al.* [1981, 1982]. Using the Voyager 1 and 2 plasma data sets Sittler *et al.* [1983] and Lazarus and McNutt [1983] presented comprehensive results on the electron and ion plasma properties, respectively. Lazarus and McNutt [1983] identified a light ion component and heavy ion components, which they identified as  $\text{H}^+$  and  $\text{O}^+$ , respectively. Richardson [1986] presented the most definitive results of the Voyager 1 and 2 ion fluid parameters. These were later followed by Richardson and Sittler [1990], who combined the fluid parameter results from Sittler *et al.* [1983] for electrons with those of Richardson [1986] for ions. Richardson and Sittler [1990] took into account spacecraft charging corrections. They then solved the field-aligned force balance equation to compute 2-D maps ( $r, \lambda$ ) of the ion and electron fluid parameters.

[3] Young *et al.* [2005] presented initial results recorded by the CAPS instrument during the first Cassini orbit. In this paper we expand those results by presenting ion and electron fluid parameters taken at  $L > 3$  during the Cassini approach trajectory before Saturn Orbit Insertion (SOI). During SOI the spacecraft approached and exited Saturn's magnetosphere at mid-latitudes ( $\lambda \sim -15^\circ$ ) similar to Voyager 2 with ring plane crossings between the F and G rings ( $L \sim 2.7$ ). Therefore, we cannot make a complete comparison with Voyager. In order to solve the field-aligned force balance equation, equatorial orbits, which will occur later in the tour, are required. Here we present fluid measurements for both protons ( $\text{H}^+$ ) and water group ions (including  $\text{O}^+$ ,  $\text{OH}^+$ ,  $\text{H}_2\text{O}^+$  and  $\text{H}_3\text{O}^+$ , which we designate as  $\text{W}^+$ ). The analysis is confined to the inbound portion of the trajectory because the viewing of the corotating flow direction was not optimal on the outbound leg.

### 2. Ion Composition Measurements

[4] The CAPS instrument [Young *et al.*, 2004] is composed of three separate particle instruments: Ion Mass Spectrometer (IMS), Electron Spectrometer (ELS) and an Ion Beam Spectrometer (IBS). The IMS, which makes 62 contiguous ion measurements between 1 volt and 50 kV in E/Q with resolution of 17%, has a composition capability for which it uses time-of-flight (TOF) technology. It has an

<sup>1</sup>NASA Goddard Space Flight Center, Greenbelt, Maryland, USA.

<sup>2</sup>Los Alamos National Laboratory, New Mexico, USA.

<sup>3</sup>Engineering Physics, University of Virginia, Charlottesville, Virginia, USA.

<sup>4</sup>Mullard Space Science Laboratory, University College London, Dorking, UK.

<sup>5</sup>Southwest Research Institute, San Antonio, Texas, USA.

<sup>6</sup>Department of Physics and Astronomy, University of Montana, Missoula, Montana, USA.

<sup>7</sup>Blackett Laboratory, Imperial College, London, UK.

<sup>8</sup>Centre d'Etude Spatiale des Rayonnements, Toulouse, France.

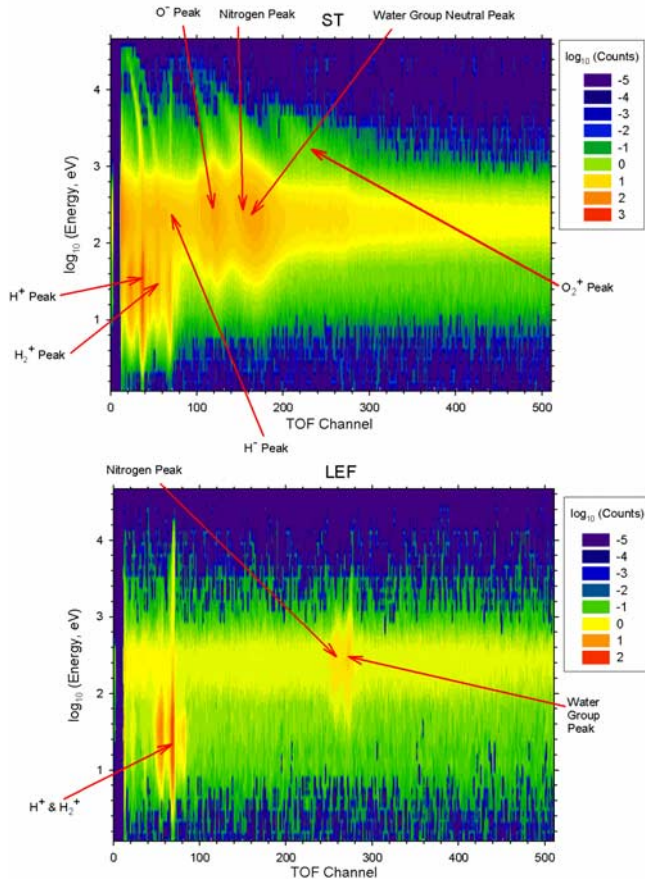


**Figure 1.** Energy-TOF color spectrogram of summed ion counts for ST and LEF for the time period analysis was done. Ion fragment peak identifications are indicated.

intermediate mass resolution capability that produces Straight Through (ST) data and a high mass resolution capability that produces Linear Electric Field (LEF) data. The latter technique has the ability to separate molecular species of the same  $M/Q$  [Young *et al.*, 2004]. Young *et al.* [2005] first reported that within the inner magnetosphere ion population is dominated by protons and water group ions ( $O^+$ ,  $OH^+$ ,  $H_2O^+$ ,  $H_3O^+$ ) with minor constituents of  $N^+$  ( $\sim 5\%$ ) and  $O_2^+$  ( $\sim 1-2\%$ ). In addition,  $O_2^+$  and  $O^+$  are dominant species over Saturn's rings. A more detailed analysis of the  $N^+$  results is given by Smith *et al.* [2005].

[5] In Figure 1 we show  $E/Q$  versus TOF spectrograms of coincident ion counts summed over the six hour period (SCET 182:1800–2400 hours on June 30, 2004) for which we have analyzed the ion measurements and computed fluid parameters (i.e., density, flow velocity, temperature) for both ions and electrons. The ST data shows the presence of  $H^+$  and water group ions with minor species of  $H_2^+$ ,  $N^+$  and  $O_2^+$ . The LEF data clearly shows the presence of a well resolved  $N^+$  peak. The detection of  $N^+$  was one of the possibilities that Johnson and Sittler [1990] and Sittler *et al.* [2004] predicted due to primordial  $NH_3$  in the surface ice of the various icy moons of Saturn [Delitsky and Lane, 2002]. The  $N^+$  could also come from a neutral nitrogen torus around Titan's orbit that can extend into the inner magnetosphere [Smith *et al.*, 2004]. The spectrograms also show

the presence of self-induced background tails and background due to Saturn's radiation belts inside of Enceladus' orbit. For our fluid calculations we have approximately corrected for the tails by comparing the amplitude of the tails relative to that for the main  $W^+$  peaks in the TOF spectra and then subtracted this fraction from the measured ion counts. There are several minor peaks that have not yet been determined and will be analyzed later. However, they have no impact on results presented here. During data acquisition the IMS bins the coincident ion counts within TOF buckets for the protons, each of the water group ions,  $C^+$  and  $N^+$ . The ion counts are derived from an on-board deconvolution algorithm that is applied to the TOF data [Sittler, 1993] via the instruments Spectrum Analyzer Module (SAM) [Young *et al.*, 2004]. Due to slight misalignments of the TOF buckets the estimated onboard ion counts weren't correct, but by summing the water group ions on the ground, the effect of the misalignments tended to cancel out and give the correct water group flux. Coincident ion counts, are measured over the full energy range and 8 angular sectors over a field-of-view (FOV) of  $160^\circ$  with a resolution of  $8^\circ \times 20^\circ$  [Young *et al.*, 2004]. The FOV is aligned parallel to the spacecraft Z-axis and can be actuated over a range of  $\sim 180^\circ$  perpendicular to the axis. However, during this particular period, the actuator was in a fixed position, so that our measurements are essentially 2D in velocity space. For simplicity we will only be presenting fluid parameters for  $H^+$  and  $W^+$ . The data were analyzed at a time resolution  $\sim 32$  seconds for ions and  $\sim 2$  seconds for electrons.

### 3. Fluid Parameter Results

#### 3.1. Analysis

[6] The fluid parameters were computed using a quasi-moment technique where the ion flux for each species was set to zero in the plasma frame of reference. We assumed a mean mass ( $m$ ) = 17 AMU for the  $W^+$  ions. This was done by taking the first order velocity moment of each species, adjusting the flow velocity in a Saturn inertial frame (i.e., removed spacecraft velocity in Saturn frame), shifting the velocity of each data point into the proper frame, and then taking the mirror image of each data point in the proper frame (i.e., we assume gyrotropy). We also make sure double counting in velocity space does not occur. The data are then mapped out of the collimator plane of the instrument (i.e., we assume the ion distribution is isotropic) so that we can approximate the  $4\pi$  coverage needed for our moment integrations. We know that the isotropy approximation is violated in a number of regions and this will be corrected in the future. The 2D velocity space "frame" is that defined by the instrument collimator. We define the flow velocities in terms of a Saturn centered cylindrical coordinate system ( $V_R$ ,  $V_\phi$ ,  $V_Z$ ). Since the measurements are effectively 2D, and since the instruments FOV is tilted  $\sim 38^\circ$  from the equatorial plane the azimuthal velocity  $V_\phi$  and cylindrical radial velocity  $V_R$  are more constrained, while  $V_Z$  is less constrained. Using Voyager data Richardson [1986] determined that  $V_Z \sim 0$  km/s within Saturn's inner magnetosphere and when combined with the weak coupling for  $V_Z$ , we would expect  $V_Z \sim 0$  km/s, which is essentially what we get. Once the flow velocity is known, we can compute the zeroth-order moment in the proper frame for

the ion density  $N_i$  and take the second moment in the proper frame to compute the ion pressure  $P_i$ . Then by taking the ratio of  $P_i$  and  $N_i$  we can get an estimate of the ion temperature  $T_i$  (i.e.,  $T_i = P_i/(N_i k_B)$ , where  $k_B$  is Boltzmann's constant). We also have the capability to shift each data point in energy space by the spacecraft potential  $\Phi_{sc}$  along the radial direction relative to the center of the spacecraft (i.e., we assume the Debye Length  $\lambda_D$  of the plasma and photo-electrons is much larger than the dimensions of the spacecraft). This allows us to take into account the effect of spacecraft charging on the fluid calculations.

### 3.2. Results

[7] In Figure 2 we show the results of our fluid calculations as plots of ion number density  $N_i$ , ion flow velocity (i.e.,  $V_R$ ,  $V_\phi$ ), and ion temperature  $T_i$  for both protons (red trace) and water group ions (blue trace). We also show the total ion number density, which should be equal to the electron number density (i.e.,  $N_H + N_W = N_e$ ). Alignment is such that we only measure  $T_\perp$  and by assuming isotropy overestimate  $N_H$ ,  $N_W$  by  $\sqrt{T_\perp/T_\parallel}$ . Therefore, we assume  $T_\perp/T_\parallel \sim 2$  for  $H^+$  and  $T_\perp/T_\parallel \sim 5$  for  $W^+$  based on *Richardson and Sittler* [1990]. In the outer regions near Rhea, where the presence of trapped photoelectrons in the ELS energy spectra indicated a positive spacecraft potential,  $\Phi_{sc} > 0$  volts, the calculated total ion density and the calculated electron density agree to within present uncertainties in their respective geometric factors.

[8] Near the orbit of Rhea, the spacecraft latitude is such that it is above the centrifugally confined inner plasmasphere, and the densities for  $H^+$  and  $W^+$  are comparable. Inside Dione's L shell, when the spacecraft starts to dip into the plasmasphere, the  $W^+$  ions start to dominate, reaching densities  $\sim 40 \text{ cm}^{-3}$  just outside of Mimas' L shell, while the proton densities reach a plateau and then decrease as the spacecraft nears the ring plane. This feature is consistent with centrifugal confinement of the heavy ion component, whereas, because of the ambipolar electric field the protons tend to float above the ring plane.

[9] In the third panel of Figure 2, the derived azimuthal velocity of the water group ions is very close to corotation, but the protons appear to be super-corotating. This feature (apparent super-rotation) could be due to a probable negative spacecraft potential, which has been neglected for the calculations presented in Figure 2. A spacecraft potential of  $\sim -2$  to  $-5$  volts is consistent with the electron observations. Including it in the calculation brings the derived  $H^+$  flow velocity to very near corotation. A spacecraft potential of this magnitude also reduces the apparent disparity between the derived ion and electron densities, which is evident in Figure 2. The  $W^+$  velocity is relatively unaffected by such potentials (i.e.,  $H^+$  energies  $\sim 10 \text{ eV} \sim e\Phi_{sc}$ , while  $W^+$  energies  $\sim 250 \text{ eV} \gg e\Phi_{sc}$ ).

[10] In the second panel of Figure 2 the protons have a temperature  $T_H \sim 10 \text{ eV}$  near Rhea which then steadily decreases with decreasing radial distance such that  $T_H \sim 2 \text{ eV}$  just outside Mimas' L shell. The rise in temperature toward 2400 SCET occurs due to the loss of the cold ion beam and we only see the hot component. Since the Voyager plasma instrument had a low energy cut-off of 10 eV and CAPS can provide measurements down to  $\sim 1 \text{ eV}$ , these results are the first measurements of proton temperatures and densities

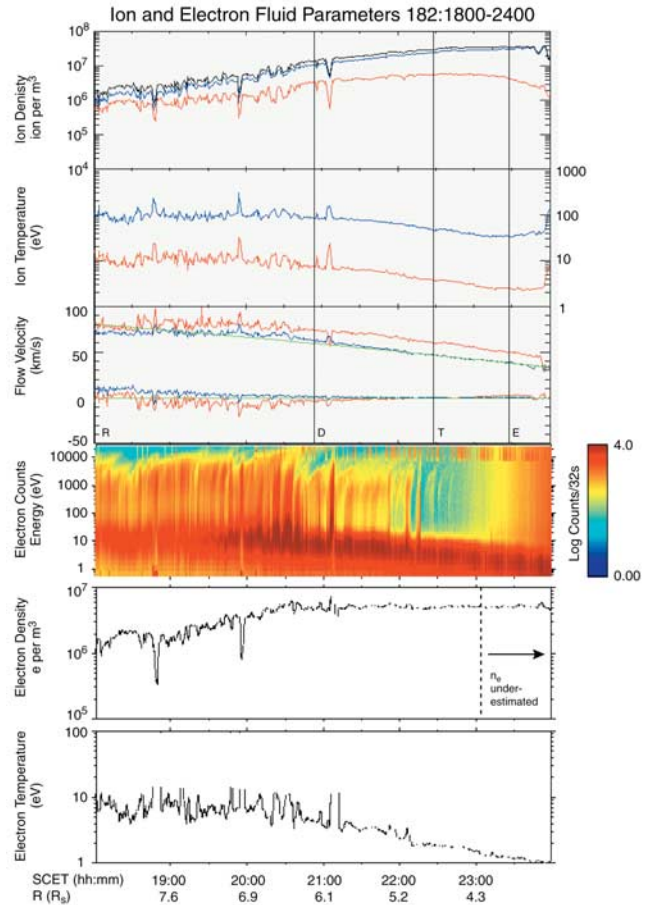


**Figure 2.** In the upper three panels ion fluid parameters number density, temperature and flow velocity are displayed for protons (red) and water group ions (blue). Total ion density indicated in black. With regard to the flow velocity the corotation speed for azimuthal flow is indicated by the upper green line and the lower green line is for the cylindrical radial velocity to equal zero. The fourth panel shows energy-time color spectrogram for electron measurements, the fifth panel shows thermal electron number density and the lower panel shows the thermal electron temperature. The horizontal axis is the observation time in spacecraft event time (SCET). The vertical lines labeled R, D, T and E indicate the times when the spacecraft crossed the dipole L shells of the moons Rhea, Dione, Tethys and Enceladus, respectively. Statistical errors are  $\sim 5\%$  at Rhea's L shell and decrease to  $\sim 1\%$  for  $W^+$  and  $\sim 2\%$  for  $H^+$  inside of Dione's L shell. Systematic errors  $\sim +20\%$  are estimated for the density,  $< 8\%$  for the flow and  $\sim +7\%$  for the temperature.

within the inner most regions of Saturn's magnetosphere. It is also interesting to note that the temperature of the protons  $T_H$  was approximately equal to the thermal electron temperature  $T_{ec}$  (i.e.,  $T_H \sim T_{ec}$ ). Water group ion temperatures are  $T_W \sim 100 \text{ eV}$  near Rhea's L shell and then systematically decrease with decreasing radial distance to about  $T_W \sim 40 \text{ eV}$  just outside Mimas' L shell. These results are qualitatively equivalent to those computed by *Richardson* [1986] using the Voyager plasma

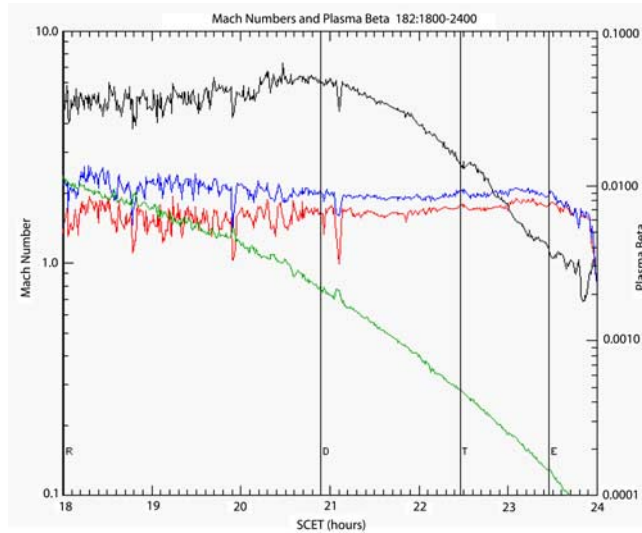


**Figure 3.** The Alfvén Mach number (green), Sonic Mach number for protons (red) and water group ions (blue) and plasma beta (black) versus time derived from data in Figure 2. Uncertainties are at most  $\sim 10\%$  for the Mach numbers and  $\sim 20\%$  in an absolute sense for the plasma beta.

data. Referring to the fourth panel of Figure 2, note that the hot electron component drops drastically inside Tethys' L shell where significant amounts of neutral oxygen have been observed [Esposito *et al.*, 2005]. In addition, the energetic particle populations reported by Krimigis *et al.* [2005] are severely depleted within the same region. For times after 2300 SCET there is evidence of penetrating radiation in the electron spectrogram.

#### 4. Conclusions

[11] The centrifugally confined plasma will impose stresses on Saturn's magnetic field and contribute to its ring current as originally reported by Connerney *et al.* [1981]. This can be understood by the following equation from Sittler *et al.* [1983] for a dipole field:

$$j_{\perp} = \frac{1}{4\pi} \left( \frac{B_0}{r_0} \right) M_{A0}^2 \left[ R^{-(\alpha-4)} + \frac{(\alpha-\delta)}{2} \frac{1}{M_{S0}^2} R^{-(\alpha-\delta-2)} \right] \quad (1)$$

with  $r_0$  a reference point in  $r$ ,  $B_0 = B(r_0)$ ,  $N_e \sim 1/R^{\alpha}$  and  $T \sim R^{\delta}$ . This equation shows that the ring current is proportional to the Alfvén Mach number  $M_A$  squared and a second term proportional to  $(M_A/M_S)^2 = \beta^2$  where  $M_S$  is the Sonic Mach number and  $\beta$  is the plasma beta. Therefore, in regions where  $M_A$  and  $\beta$  are greater than 1 the stress terms will be significant and result in an observable ring current. In Figure 3 we show plots of the Alfvén Mach number (green), Sonic Mach number for protons (red), Sonic Mach number for water group ions (blue) and the plasma beta (black) for our analysis interval. In the outer region  $M_A > 1$  occurs and centrifugal effects should be important, while the Sonic Mach numbers for  $H^+$  and  $W^+$  are generally greater than one and the plasma beta  $\beta \ll 1$ . Therefore, pressure gradient terms are small. In the case of the Voyager 1 ring plane crossing at Dione's L shell  $\beta \sim 1$  (E. C. Sittler Jr. *et al.*,

Energetic nitrogen ions within the inner magnetosphere of Saturn, submitted to *Journal of Geophysical Research*, 2004) so that pressure gradient terms were important at that time. This difference can be traced to the fact that Cassini SOI trajectory was generally above the plasma sheet. Most of the heavy ions that dominate both centrifugal and pressure forces on the plasma are confined to the equatorial plane. An orbit through the equatorial magnetosphere, planned for later in the tour, will be required to determine the true stress balance on the magnetosphere caused by the rotating flow.

[12] We have presented the first estimates of the ion fluid parameters from the CAPS instrument for Saturn's inner plasmasphere. They are qualitatively consistent with that estimated from Voyager plasma measurements. In addition we have determined the low temperatures of protons and electrons within the inner magnetosphere which Voyager could not determine.

[13] **Acknowledgments.** We acknowledge the contributions by Sarabjit Bakshi (SSAI), Don Glenn (SSD), Kevin Edwards (SSD), Michael Johnson (GSFC) and Ezinne Uzo-Okoro (GSFC). We also acknowledge the rest of the CAPS team and the support by NASA/JPL under contract 1243218 with SwRI. Work at Los Alamos was performed under the auspices of the U.S. Dept. of Energy. Work at MSSL was funded by PPARC.

#### References

- Bridge, H. S., *et al.* (1981), Plasma observations near Saturn: Initial results from Voyager 1, *Science*, 212, 217.
- Bridge, H. S., *et al.* (1982), Plasma observations near Saturn: Initial results from Voyager 2, *Science*, 215, 563.
- Connerney, J. E. P., M. H. Acuna, and N. F. Ness (1981), Saturn's ring current and inner magnetosphere, *Nature*, 292, 724.
- Delitsky, M. L., and A. L. Lane (2002), Saturn's inner satellites: Ice chemistry and magnetosphere effects, *J. Geophys. Res.*, 107(E11), 5093, doi:10.1029/2002JE001855.
- Esposito, L. W., *et al.* (2005), Ultraviolet imaging spectroscopy shows an active Saturnian system, *Science*, 307, 1251.
- Frank, L. A., B. G. Burek, K. L. Ackerson, J. H. Wolfe, and J. D. Mihalov (1980), Plasmas in Saturn's magnetosphere, *J. Geophys. Res.*, 85, 5695.
- Johnson, R. E., and E. C. Sittler Jr. (1990), Sputter-produced plasma as a measure of satellite surface composition: The Cassini mission, *Geophys. Res. Lett.*, 17, 1629.
- Krimigis, S. M., *et al.* (2005), The dynamic Saturn magnetosphere: First results from Cassini/MIMI, *Science*, 307, 1270–1273.
- Lazarus, A. J., and R. L. McNutt Jr. (1983), Low-energy plasma ion observations in Saturn's magnetosphere, *J. Geophys. Res.*, 88, 8831.
- Richardson, J. D. (1986), Thermal ions at Saturn: Plasma parameters and implications, *J. Geophys. Res.*, 91, 1381.
- Richardson, J. D., and E. C. Sittler Jr. (1990), A plasma density model for Saturn based on Voyager observations, *J. Geophys. Res.*, 95, 12,019.
- Sittler, E. C., Jr. (1993), Real-time spectral analysis algorithm for space plasma three-dimension ion mass spectrometers, *Rev. Sci. Instrum.*, 64, 2771.
- Sittler, E. C., Jr., K. W. Ogilvie, and J. D. Scudder (1983), Survey of low-energy plasma electrons in Saturn's magnetosphere: Voyagers 1 and 2, *J. Geophys. Res.*, 88, 8847.
- Sittler, E. C., Jr., R. E. Johnson, S. Jurac, J. D. Richardson, M. McGrath, F. Crary, D. T. Young, and J. E. Nordholt (2004), Pickup ions at Dione and Enceladus: Cassini plasma spectrometer simulations, *J. Geophys. Res.*, 109, A01214, doi:10.1029/2002JA009647.
- Smith, H. T., R. E. Johnson, and V. I. Shematovich (2004), Titan's atomic and molecular nitrogen tori, *Geophys. Res. Lett.*, 31, L16804, doi:10.1029/2004GL020580.
- Smith, H. T., M. Shappirio, E. C. Sittler, D. Reisenfeld, R. E. Johnson, R. A. Baragiola, F. J. Crary, D. J. McComas, and D. T. Young (2005), Discovery of nitrogen in Saturn's inner magnetosphere, *Geophys. Res. Lett.*, 32, L14S03, doi:10.1029/2005GL022654.
- Wolfe, J. H., J. D. Mihalov, H. R. Collard, D. D. McKibbin, L. A. Frank, and D. S. Intriligator (1980), Preliminary results on the Plasma environment of Saturn from the Pioneer 11 plasma analyzer experiment, *Science*, 207, 403.

Young, D. T., et al. (2004), Cassini plasma spectrometer investigation, *Space Sci. Rev.*, 114, 1–112.

Young, D. T., et al. (2005), Composition and dynamics of plasma in Saturn's magnetosphere, *Science*, 307, 1262.

---

N. Andre, Centre d'Etude Spatiale des Rayonnements, Toulouse F-31028, France.

D. Chornay, M. D. Shappirio, D. Simpson, and E. C. Sittler Jr., NASA Goddard Space Flight Center, Greenbelt, MD 20771, USA. (edward.c.sittler@nasa.gov)

A. J. Coates and A. M. Rymer, Mullard Space Science Laboratory, University College London, Holmbury St. Mary, Dorking, Surrey RH5 6NT, UK.

F. Crary, D. J. McComas, and D. T. Young, Southwest Research Institute, San Antonio, TX 78228, USA.

M. Dougherty, Blackett Laboratory, Imperial College, London SW7 2BZ, UK.

R. E. Johnson and H. T. Smith, Engineering Physics, University of Virginia, Charlottesville, VA 22904, USA.

D. Reisenfeld, Department of Physics and Astronomy, University of Montana, Missoula, MT 59812, USA.

M. Thomsen, Los Alamos National Laboratory, NM 87545, USA.